AIP Conference Proceedings

Synthesis of nanoparticles by laser ablation from heat-treated porous silicon for biomedical applications

Cite as: AIP Conference Proceedings **2380**, 040002 (2021); https://doi.org/10.1063/5.0058277
Published Online: 25 June 2021

F. K. Başak, and E. Kayahan

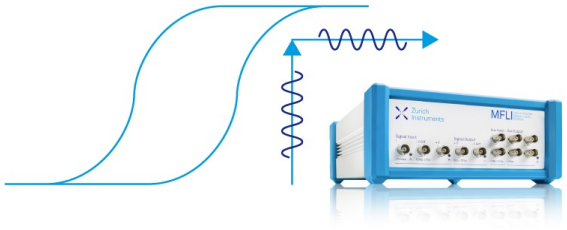
View Online Export Citation

ARTICLES YOU MAY BE INTERESTED IN

Characterization of Ta doped HfO_2 for waveguiding applications
AIP Conference Proceedings **2380**, 040006 (2021); https://doi.org/10.1063/5.0058232

Nanoencapsulated aroma finishing on fabric by sol-gel process
AIP Conference Proceedings **2380**, 040005 (2021); https://doi.org/10.1063/5.0058186

Catalytic effect of cobalt catalysts in the reaction of hydrogenation of ethylene-containing acetylene to ethylene
AIP Conference Proceedings **2380**, 020002 (2021); https://doi.org/10.1063/5.0058263



© 2021 Author(s).

Synthesis of Nanoparticles by Laser Ablation from Heat-Treated Porous Silicon for Biomedical Applications

F.K. Başak[2, 3, a)], E.Kayahan[1,2]

[1]*Kocaeli University, Electro-Optics and Systems Eng. Umuttepe, 41380, Kocaeli, Turkey*

[2]*Kocaeli University, Laser Technologies Research and Application Center, 41275, Yeniköy, Kocaeli, Turkey*

[3]*Kocaeli University, Biomedical Eng. Umuttepe, 41380, Kocaeli, Turkey*

[a)]Corresponding author:filizkarakus@gmail.com

Abstract. HPSi nanoparticles were produced for the first time from heat treated porous silicon (HPSi) by pulsed laser ablation in acetone and n-hexane liquids. Both HPSi nanoparticles and PSi (Porous silicon) and HPSi samples were analyzed by various spectroscopic methods. From the Dynamic Light Scattering (DLS) analysis, it's observed that the highest size density of Si nanoparticles is 106nm and 80 nm which produced in acetone and n-hexane, respectively. We produced silicone nanoparticles from heat treated porous silicone, which are characterized by strong Si-C bonds or strong Si-O bonds with chemically tailored surfaces by laser ablation method. In addition, the HPSi nanoparticles are ultrapure, blue luminescent and have spherical shapes as well as the desired zeta potential for biopolymer coating and other biomedical applications. Heat treatment of porous silicone before short pulse laser ablation limits the size distribution of the particles to a narrower range.

INTRODUCTION

Porous silicon (PSi) has a high surface/volume ratio, effective luminescence in the visible region at room temperature, and it is adaptable to integrated circuits. PSi is soluble in physiological liquids; its surface properties can be modified to be hydrophilic or hydrophobic; and it is excreted from our bodies as orthosilicic acid. [1]. Porous silicon is also biodegradable, easily surface functionalized, biocompatible, and can be processed into a variety of sizes such as micro or nanoparticles. In addition, it can be produced as bioactive or bioinert. Silicon is one of the most common trace elements after zinc and iron in the human body and it is effective in optimizing bone health [2]. This biomaterial can be immobilized to biomolecules by some specific methods such as covalent bonding, electrostatic interaction and adsorption. Silicon nanoparticles (SiNPs) production is a crucial process for biomedical applications that focuses on the development of intelligent drug design [3], detecting various biomolecules [4], medical imaging [5], and treating tumorous tissue through photodynamic therapy [6]. As its minimal toxic effect, SiNPs has become a promising platform for the early diagnosis and treatment of lethal diseases in the biomedical field [7].

Many methods have been developed to produce SiNPs such as electrochemical techniques [8], liquid-solution-phase synthesis [9], microwave induced deposition [10] and laser ablation [11]. Laser ablation method allows the removal of micro/nanoscale particles from a target material. Nanoparticles produced by conventional chemical methods contain various impurities due to their incorporation of nitrates such as nitrate salts, chlorides and nitrates and need to be further purified [12]. The production of silicon nanoparticles by laser ablation method enables the production of ultrapure, ligand-free and clean-surface nanoparticles [13]. Therefore, laser-produced nanoparticles are very vital for biomedical applications. In the nanosecond laser ablation process in liquids, plasma formation occurs at a high rate in materials that exhibit interactions such as multiphoton absorption and ionization [14]. The nanocrystals in the porous silicon structure exhibit multiphoton absorption and show superior ability in terms of multiphoton ionization due to their lower refractive index than bulk silicon [15].

Proceedings of the 10th International Advances in Applied Physics and Materials Science Congress & Exhibition
AIP Conf. Proc. 2380, 040002-1–040002-10; https://doi.org/10.1063/5.0058277
Published by AIP Publishing. 978-0-7354-4107-1/$30.00

The aim of this study is to investigate the properties of Si nanoparticles, synthesized from HPSi by using laser ablation method. HPSi is known to be more resistant to harsh chemical environments. According to our review of the literature, there is no report on the production of nanoparticles from HPSi using the laser ablation method. Examining both biomedical applications and toxicology studies, it was discovered that the suitable zeta potential for in vivo studies was neutral, and the preferred particle size was around 80-140nm [16, 17]. The nature of the fluids used during laser ablation affects the growth, composition and stability of nanoparticles [18]. Acetone was preferred as the liquid medium due to the high stability of the silicon nanoparticles in acetone. In addition, acetone media can be used as a solvent in coating silicone nanoparticles with biopolymers such as poly (ethylene glycol) (PEG) and poly (lactic-glycolic acid) (PLGA). n-hexane is preferred for the examination of laser ablation process with a different fluid. The nanoparticles produced in organic solvents were characterized using various spectroscopic methods described and used in this study.

EXPERIMENTAL

HPSi nanoparticles were generated by exposing HPSi targets to nanosecond laser pulses in a liquid environment. First of all, we produced HPSi for this purpose. The crystalline silicon (c-Si) wafers were cut into pieces to obtain a 1 cm² porous area. Silicon pieces were ultrasonically washed with acetone for 10 minutes. After rinsing with ethanol, they were dried on a fume hood at room temperature. Cleaned silicon pieces were placed in a teflon cell, which was then filled with a dilute H_2O (1:5) solution. PSi pieces were made from n-type 111>, Sb (antimony) doped (0.008–0.02 cm) silicon wafers by electrochemical etching at 50 mA/cm^2 for 45 minutes in a solution of (1:1) HF(38 %): Ethanol. To heat treat the PSi samples, the acetonitrile liquid was poured into the gas washing bottle, and nitrogen gas was blown into the bottle via a pipe. The PSi pieces were then heat treated for 15 minutes at 500 °C in a N_2/acetonitrile mixed gas flow and cooled to room temperature in a stream N_2 gas.

HPSi nanoparticles were generated using the laser ablation method with a nanosecond pulsed laser in high pure acetone (99.9%) and n-hexane (99.9%) liquids. The wavelength of the Nd:YAG laser is 532 nm, the pulse width is 6 ns, the frequency is 10 Hz, and the pulse energy is 60 mJ. The target material (HPSi) was placed vertically inside a pyrex beaker in the middle of the beaker. To make HPSi nanoparticles, the beaker was first filled with acetone (5ml), and then the laser beam was focused onto the target material surface with a plano convex lens (Newport model no: KPX103AR.33-focal length is 175mm). The sample was set at a distance of 95 mm from the lens. The pyrex beaker was placed on a movable platform, which was automatically moved to achieve uniform irradiation of the silicon surface and all HPSi surfaces scanned by the laser. The procedure was also repeated for n-hexane using the same experimental parameters. The nanoparticles in colloidal solution were dropped on a clean measuring plate with a syringe (ten drops), and the liquid was vaporized at room temperature to separate the nanoparticles for Scanning Electron Microscope (SEM) and measurements.
Fourier Transform Infrared (FTIR) spectroscopy was used to examine the surface bond composition and stability of the PSi and HPSi samples produced. The SEM method was used to investigate the formation of porous silicon. Photoluminescence spectroscopy was used to determine the optical properties of PSi and HPSi samples. UV-VIS spectrometry was used to characterize the optical properties of the obtained HPSi nanoparticles (Ocean 4000 spectrometer). Dynamic Light Scattering (DSL) and zeta potential analysis were performed on these nanoparticles using the Zetasizer Nano ZS to determine the surface zeta potential and particle size distribution. SEM was used to confirm the shape and distribution of the nanoparticles. Energy Dispersive X-Ray Spectroscopy was used to determine the elemental composition of the produced HPSi nanoparticles (EDS).

RESULTS AND DISCUSSION

The surface chemistry of the PSi should be adjusted to achieve a more stable PSi surface in harsh chemical environments. As a result, PSi is heat treated under specific conditions. Figure 1 shows SEM images of PSi samples before and after heat treatment (HPSi). The mesoporous PSi structure is formed in the figure, and the pore size and pore distribution have slightly changed after heat treatment; similar results are also mentioned in ref [19].

In order to showing chemical composition of the samples FTIR studies were performed. Obtained FTIR spectra of PSi-HPSi and 6 months aged PSi-HPSi are shown in Figure 3. In this figure, the peak shown between 1000 cm^{-1}-1300 cm^{-1} is attributed the Si-O-Si stretching mode. The peak is attributed to the Si-O-Si stretching mode in 1074 cm^{-1} is strong. Peaks of the Si-H_x stretching vibration were observed around 2110 cm^{-1} [20]. The peak at 2110 cm^{-1} is attributed to pure silicon monohydrate and silicon dihydrate. The 906 cm^{-1} wavelength shows the scissoring vibration of Si-H bonds [21].

The peak shown at 880 cm^{-1} indicates the presence of Si-H bonds [22]. In addition, the strong peak at 790 cm^{-1} exist which corresponds to the stretching mode of Si-C bond [23]. After the heat treatment, the peak of the Si-H_x bond and the peak of the Si-H bond have disappeared. It was also observed that the characteristic stretching peak of Si-O-Si decreased. Although the peaks of Si-C stretching vibrations have been shown to decrease, Si-C bonds are still present after heat treatment. It can be concluded that both SiO and SiC bonds are present before and after heat treatment of PSi. The heat-treated PSi has been shown to be very stable against air impurities even after 6 months, but PSi without heat treatment appears to be affected by impurities in the air.

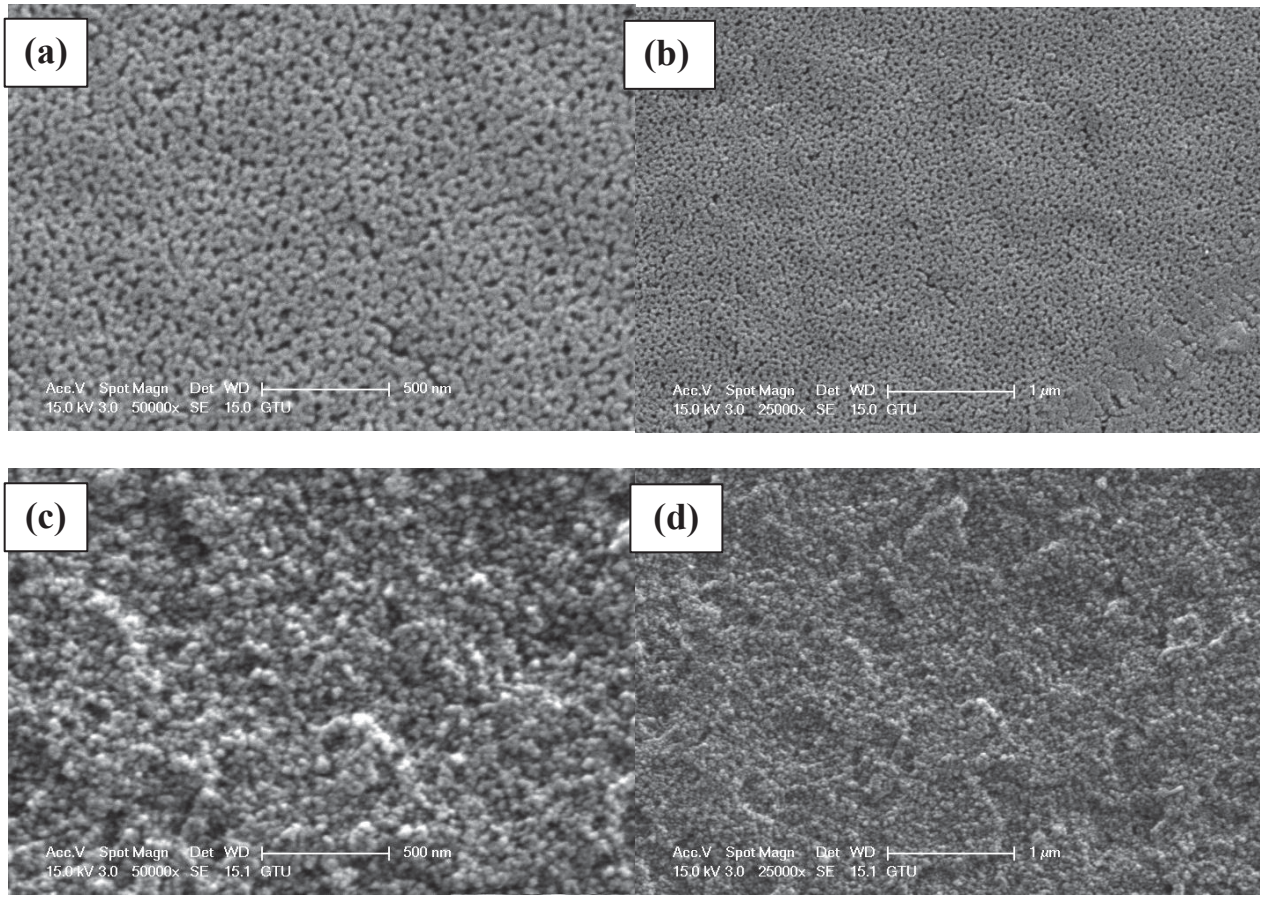


FIGURE 1. SEM images of PSi surface. Where (a), (b) are before and (c), (d) are after heat treatment.

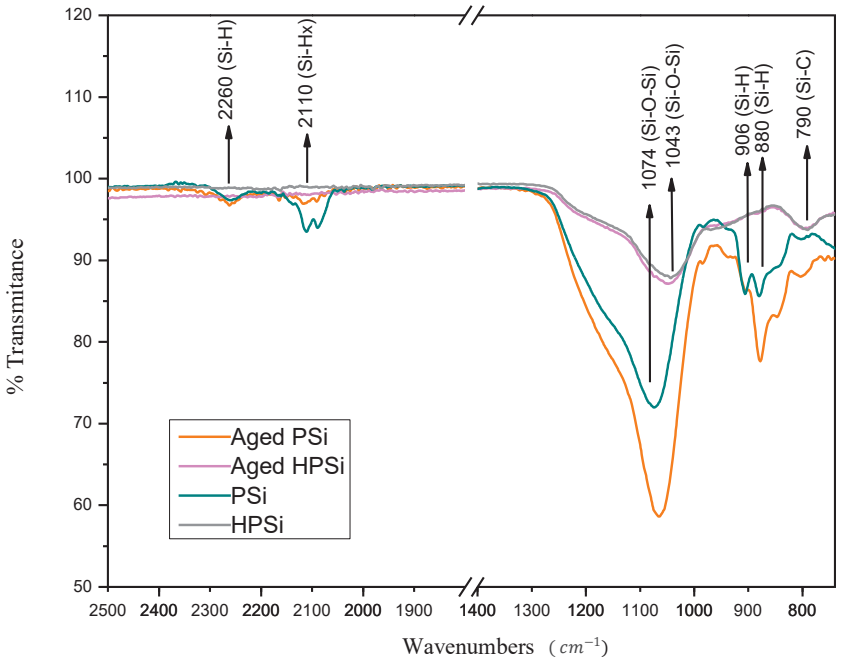


FIGURE 2. FTIR spectra of heated and as-prepared porous silicon pieces and their aged manner after 6 months.

To see PL properties of PSi before and after heat treatment, the PL spectra measurements were taken. Obtained spectra are given in Figure 2 where it is clearly shown that the PL intensity decreases after the heat treatment. The decreasing of PL intensity can be explained by the fact that H atoms leave from the PSi surface, and then the remaining dangling bonds act as a non-radiative luminescence center as mentioned in ref [24]. Besides, a previous study [25] found that silicon hydride (Si-Hx) or oxygen-based silicon hydride (OSiHx) groups were responsible for PL emissions in PSi. In this study the samples do not contain either silicon hydride (Si-Hx) or hydroxyl (SiOHx) groups after heat treatment, and this can be interpreted as the cause of the significant reduction in PL intensity. Moreover, increasing roughness on the porous layer surface after heat treatment may have caused a decrease in luminescent intensity [26].

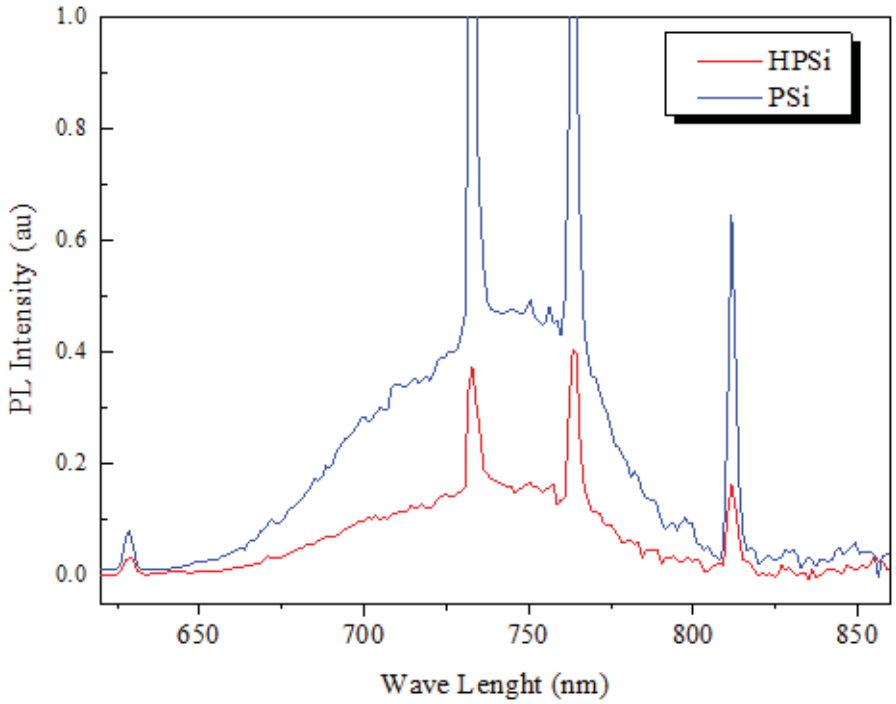


FIGURE 3. Photoluminescence spectra of PSi before and after heat treatment (HPSi).

DLS analysis was performed for silicon colloidal solution obtained by laser ablation method. For the DSL measurements, the sample solutions were deposited on a quartz omega cuvette. Particle size distribution of HPSi nanoparticles were shown in Figure 4(a) and Figure 4(b). DSL measurements showed that there was a particle size distribution ranging from 38 nm to 340 nm in acetone medium. It was found out that the nanoparticles within the distribution with the size of 106 nm had the highest rate (10.7%). The next highest size distribution was 92nm with a rate of 10.6%. In our study in which n-hexane was chosen as the liquid medium, particles size distribution was found to be ranging from 50 nm to 140 nm as a result of DLS analysis. The highest nanoparticle size distribution was found out to be 80 nm with a rate of 21.6% in n-hexane. It was also found that the next highest nanoparticle size distribution was 92 nm with a rate of 21.2% in n-hexane. Adjusting the required conditions, the desired sized nanoparticles can be separated from the solution by centrifugation or syringe type filter. In our study, we separated the micro particles in acetone medium by centrifugation. Some of the particles in the n-hexane spontaneously separated and firmly adhered to the pyrex beaker. Therefore, centrifugation was not required on particles in the n-hexane liquid medium.

The HPSi nanoparticles produced in acetone liquid were found to have an average -0.0109mV and approximately zero zeta potential. The HPSi nanoparticles produced in n-Hexane media, the particles were found to have an average -0,0864mV and approximately zero zeta potential. Zeta potential measurements were repeated three times for each sample. As it is well known that if the zeta potential of the particles in liquid medium is greater than + 30mV or less than -30mV, it can be said that they are stable [27]. Nanoparticles with a zeta potential between -10 and +10 mV are considered approximately neutral. The zeta potential plays a significant role in vivo biomedical application. Nanoparticles with neutral zeta potential are preferred instead of nanoparticles with negative and positive potential due to various reasons arising from the physiological environment. Nanoparticles with neutral potential have an agglomeration problem. Therefore, nanoparticles with neutral zeta potential become ideal materials for in vivo studies only after PEG is coated [28]. When the zeta potential is analyzed for both liquids used in our study, it is seen that the net charge is approximately neutral. The nanoparticles we produce therefore are preferable for in vivo biomedical applications.

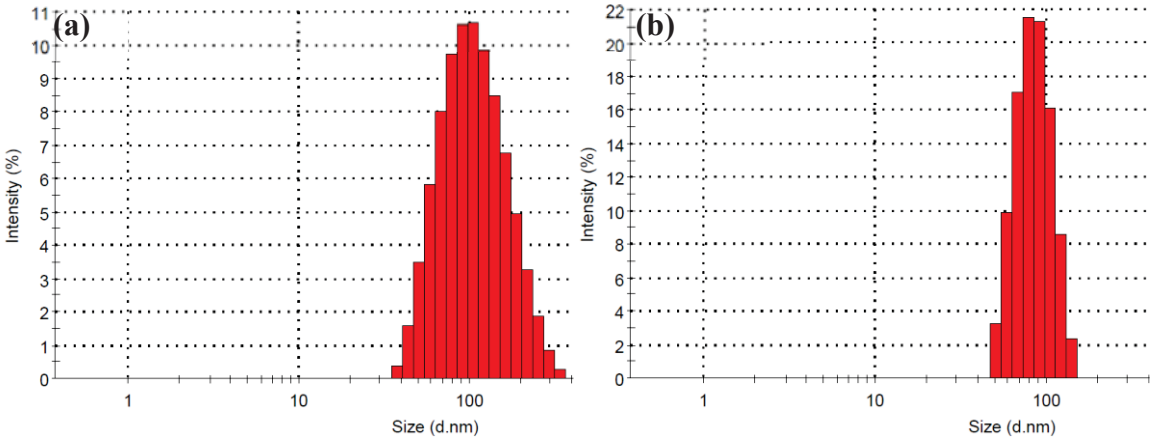


FIGURE 4. Size distribution (DLS) analysis of HPSi nanoparticles: **(a)** produced with 60mJ laser energy in acetone, **(b)** produced with 60mJ laser energy in n-hexane.

Figure 5 shows SEM images of HPSi nanoparticles. SEM measurements were taken in order to determine the shapes and sizes of the nanoparticles. According to SEM results, particles have been found to have a spherical shape. The size distribution is generally broad, from 38 nm to about 350 nm.

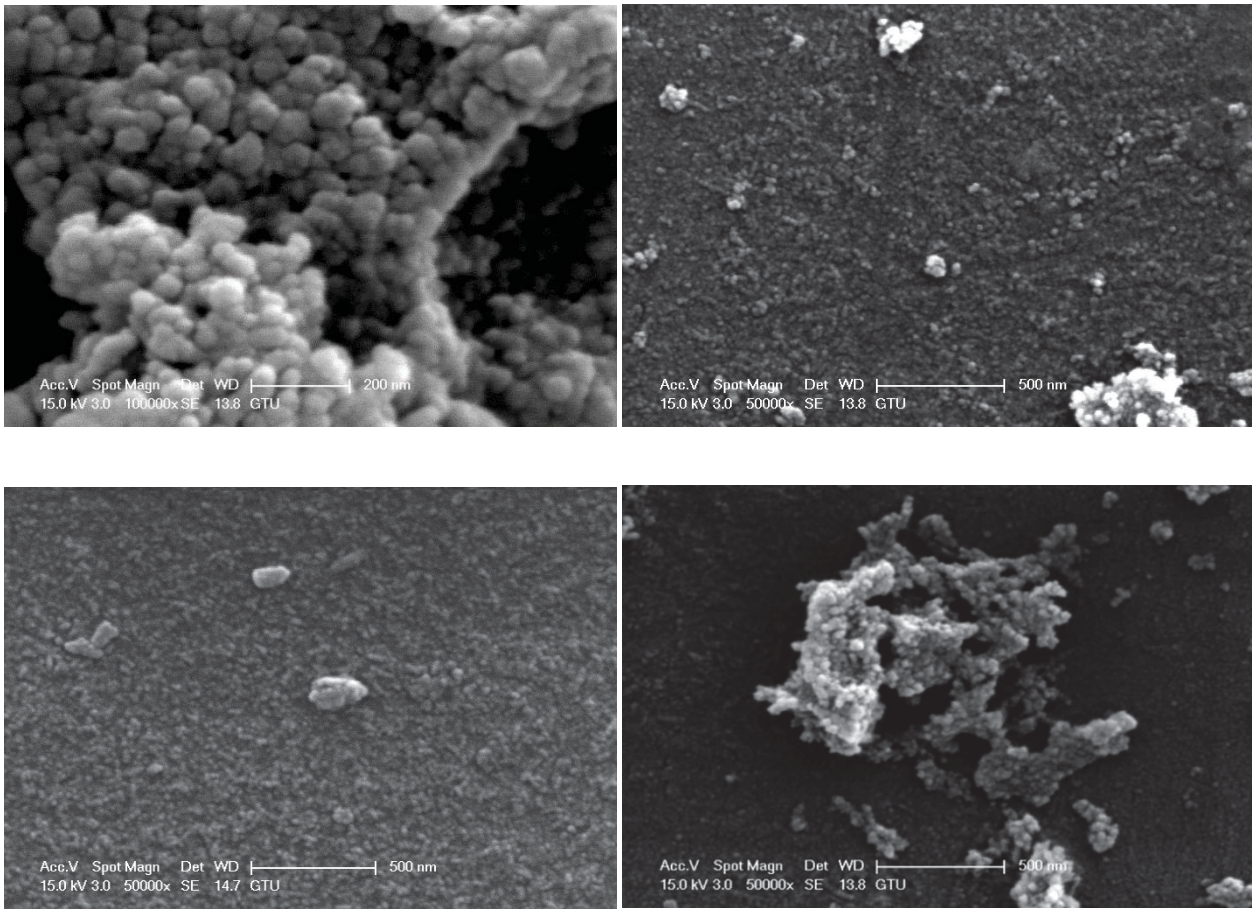


FIGURE 5. SEM images of nanoparticles produced from HPSi.

The presence of carbon atoms, as seen in the EDS spectra, proved that SiC nanoparticles were formed. In the nanoparticle solution that is the result of production, both Si, Si-O and Si-C nanoparticles are present. Si-O-Si, O-Si-H, O_3-Si-H structures that react with APTS (3-aminopropyltriethoxysilane) and GOPS (3-glycidoxypropyltrimethoxysilane) form amino (-NH group) groups that can be linked to various biomolecules. If Si-C reacts with organic compounds such as alkene and alkyne, high affinity radicals are arranged for biomolecules such as carboxyl (-COOH) on its surface [29]. Also, it can be evaluated that carbon atoms originate from both liquid medium [30] and heat treatment. In addition, the presence of atoms such as magnesium (Mg), calcium (Ca), sodium (Na), and gold (Au) has been identified. The observed peaks related to Mg, Ca, and Na are associated with the measuring plaque from which the samples were dripped before EDS analysis. The presence of Au results from the gold plating of the samples before EDS analysis.

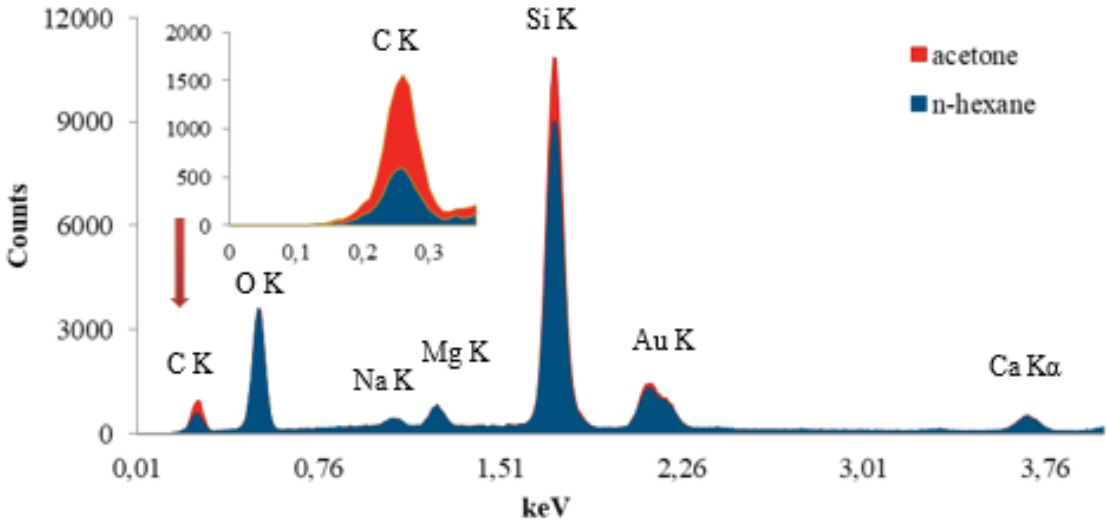


FIGURE 6. EDS spectra of HPSi nanoparticles produced in various liquids.

The UV-VIS absorbance spectra of the produced nanoparticles are given in Figure 7. The characteristic UV-VIS absorbance of the HPSi nanoparticles is in the range of 400-450 nm. It has been detected that the produced silicon nanoparticles absorb in the visible region. The colloidal solutions of Si nanoparticles present an absorption in the UV-VIS region [31]. There is no obvious correlation between size and maximum absorption. The absorption in the visible region is ascribed to the quantum size effect that occurs on the bandgap. It is certain that not the general size of nanoparticles in solution but mostly the size of nanocrystallized nanoparticles determine the absorption band. Furthermore, when looking at the size distributions obtained with a short-pulsed laser, it can be said that these particles have a polycrystalline structure [32]. In the short pulse laser regime, nanoparticles that we produce in acetone liquid medium can be in a higher polycrystalline population. After laser ablation of HPSi in liquid media, color measurements of the resulting solution were taken with a UV-VIS spectrometer. The solution was found to be light orange in accordance with its peers in the literature.

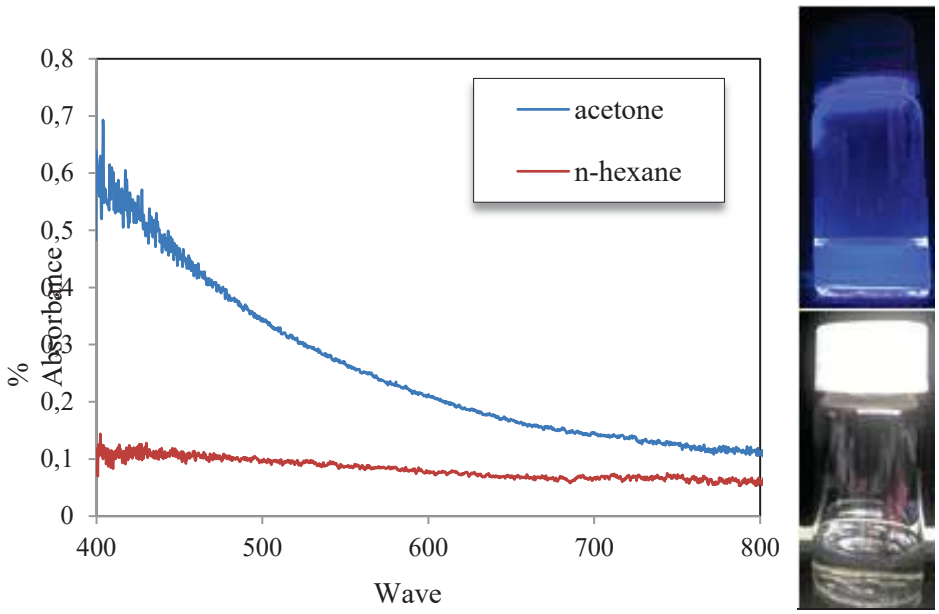


FIGURE 7. UV-VIS Absorbance spectra of HPSi nanoparticles produced in different liquids (acetone and n-hexane)

CONCLUSIONS

Porous silicone is a more advantageous biomaterial than bulk silicone, as its surface can be regulated by heat treatment and the pore size can be adjusted, thus allowing the resulting nanoparticle size to be reduced to the preferred size. Considering the zeta potential measurement, the fact that the particles have a nearly neutral charge indicates that the particles preferred for the physiological environment are produced. This structure has high interactions in physiological ambient and exhibit high endocytosis efficiency. In general, the use of acetone instead of n-hexane resulted in smaller and highly polycrystalline particles population. The use of the laser ablation method in combination with heat treatment resulted in regulated surfaces characterized by strong Si-C bonds or strong Si-O bonds. Combining the laser ablation method with heat treatment, we produced ultrapure silicon nanoparticles with chemically tailored surfaces. As a result of this study, nanoparticles of favored size and with surface charge have been produced for therapeutic applications, and these nanoparticles have a high density. In this study, we report that the PSi nanoparticles we produce for in vivo biomedical applications have chemically tailored surfaces, blue luminescent, biocompatible charge and are mostly of the preferred nanoscale for biomedical applications.

ACKNOWLEDGEMENTS

Competing interests: None declared

Funding: This study was supported by Kocaeli University Scientific Research Projects Coordination Unit [Kocaeli Uni. Project No. 2019/074 and 2016/068] and Kocaeli University Laser Technologies Research and Application Center.

Ethical approval: Not required

REFERENCES

1. J.H. Park, L. Gu, G. Von Maltzahn, E. Ruoslahti, S.N. Bhatia, M.J. Sailor, Biodegradable luminescent porous silicon nanoparticles for in vivo applications, Nat. Mater. 8 (2009) 331–336. https://doi.org/10.1038/nmat2398.
2. R. Jugdaohsingh, Silicon and bone health, J. Nutr. Heal. Aging. 11 (2007) 99–110.
3. P.J. Kinnari, M.L.K. Hyvönen, E.M. Mäkilä, M.H. Kaasalainen, A. Rivinoja, J.J. Salonen, J.T. Hirvonen, P.M. Laakkonen, H.A. Santos, Tumour homing peptide-functionalized porous silicon nanovectors for cancer therapy, Biomaterials. 34 (2013) 9134–9141 https://doi.org/10.1016/j.biomaterials.2013.08.034.

4. C.F. Wang, M.P. Sarparanta, E.M. Mäkilä, M.L.K. Hyvönen, P.M. Laakkonen, J.J. Salonen, J.T. Hirvonen, A.J. Airaksinen, H.A. Santos, Multifunctional porous silicon nanoparticles for cancer theranostics, Biomaterials. 48 (2015) 108–118. https://doi.org/10.1016/j.biomaterials.2015.01.008.
5. L. Gu, D.J. Hall, Z. Qin, E. Anglin, J. Joo, D.J. Mooney, S.B. Howell, M.J. Sailor, In vivo time-gated fluorescence imaging with biodegradable luminescent porous silicon nanoparticles, Nat. Commun. 4 (2013) 1–7. https://doi.org/10.1038/ncomms3326.
6. D.K. Chatterjee, L.S. Fong, Y. Zhang, Nanoparticles in photodynamic therapy: An emerging paradigm, Adv. Drug Deliv. Rev. 60 (2008) 1627–1637. https://doi.org/10.1016/j.addr.2008.08.003.
7. A. Correia, M.A. Shahbazi, E. Mäkilä, S. Almeida, J. Salonen, J. Hirvonen, H.A. Santos, Cyclodextrin-Modified Porous Silicon Nanoparticles for Efficient Sustained Drug Delivery and Proliferation Inhibition of Breast Cancer Cells, ACS Appl. Mater. Interfaces. 7 (2015) 23197–23204. https://doi.org/10.1021/acsami.5b07033.
8. J.H. Ahire, Q. Wang, P.R. Coxon, G. Malhotra, R. Brydson, R. Chen, Y. Chao, Highly luminescent and nontoxic amine-capped nanoparticles from porous silicon: synthesis and their use in biomedical imaging, ACS applied materials & interfaces. 4 (2012) 3285-3292. https://doi.org/10.1021/am300642m
9. J.R. Heath, A liquid-solution-phase synthesis of crystalline silicon, Science (80-.). 258 (1992) 1131–1133. https://doi.org/10.1126/science.258.5085.1131.
10. J. Knipping, H. Wiggers, B. Rellinghaus, P. Roth, D. Konjhodzic, C. Meier, Synthesis of high purity silicon nanoparticles in a low pressure microwave reactor, J. Nanosci. Nanotechnol. 4 (2004) 1039–1044. https://doi.org/10.1166/jnn.2004.149.
11. T. Yoshida, S. Takeyama, Y. Yamada, K. Mutoh, Nanometer-sized silicon crystallites prepared by excimer laser ablation in constant pressure inert gas, Appl. Phys. Lett. 68 (1996) 1772–1774. https://doi.org/10.1063/1.116662.
12. S.K. Balasubramanian, L. Yang, L.Y.L. Yung, C.N. Ong, W.Y. Ong, L.E. Yu, Characterization, purification, and stability of gold nanoparticles, Biomaterials. 31 (2010) 9023–9030. https://doi.org/10.1016/j.biomaterials.2010.08.012.
13. P. Blandin, K.A. Maximova, M.B. Gongalsky, J.F. Sanchez-Royo, V.S. Chirvony, M. Sentis, V.Y. Timoshenko, A. V. Kabashin, Femtosecond laser fragmentation from water-dispersed microcolloids: Toward fast controllable growth of ultrapure Si-based nanomaterials for biological applications, J. Mater. Chem. B. 1 (2013) 2489–2495. https://doi.org/10.1039/c3tb20285b.
14. G.W. Yang, Laser ablation in liquids: Applications in the synthesis of nanocrystals, Prog. Mater. Sci. 52 (2007) 648–698. https://doi.org/10.1016/j.pmatsci.2006.10.016.
15. R. Rankin, N.H. Burnett, P.B. Corkum, C.E. Capjack, Refraction effects associated with multiphoton ionization and ultrashort-pulse laser propagation in plasma waveguides, Opt. Lett. 16 (1991) 835. https://doi.org/10.1364/ol.16.000835.
16. S. Bhattacharjee, I.M.C.M. Rietjens, M.P. Singh, T.M. Atkins, T.K. Purkait, Z. Xu, S. Regli, A. Shukaliak, R.J. Clark, B.S. Mitchell, G.M. Alink, A.T.M. Marcelis, M.J. Fink, J.G.C. Veinot, S.M. Kauzlarich, H. Zuilhof, Cytotoxicity of surface-functionalized silicon and germanium nanoparticles: The dominant role of surface charges, Nanoscale. 5 (2013) 4870–4883. https://doi.org/10.1039/c3nr34266b.
17. M.H. Kafshgari, B. Delalat, W.Y. Tong, F.J. Harding, M. Kaasalainen, J. Salonen, N.H. Voelcker, Oligonucleotide delivery by chitosan-functionalized porous silicon nanoparticles, Nano Res. 8 (2015) 2033–2046. https://doi.org/10.1007/s12274-015-0715-0.
18. G. Cristoforetti, E. Pitzalis, R. Spiniello, R. Ishak, F. Giammanco, M. Muniz-Miranda, S. Caporali, Physico-chemical properties of Pd nanoparticles produced by Pulsed Laser Ablation in different organic solvents, Appl. Surf. Sci. 258 (2012) 3289–3297. https://doi.org/10.1016/j.apsusc.2011.11.084.
19. A.E. Pap, K. Kordás, G. Tóth, J. Levoska, A. Uusimäki, J. Vähäkangas, S. Leppävuori, T.F. George, Thermal oxidation of porous silicon: Study on structure, Appl. Phys. Lett. 86 (2005). https://doi.org/10.1063/1.1853519.
20. I. Leontis, A. Othonos, A.G. Nassiopoulou, Structure, morphology, and photoluminescence of porous Si nanowires: Effect of different chemical treatments, Nanoscale Res. Lett. 8 (2013) 1–7. https://doi.org/10.1186/1556-276X-8-383.
21. J.D. Hwang, C.H. Chou, On the origin of leakage current reduction in TiO2 passivated porosus silicon Schottky-barrier diode, Appl. Phys. Lett. 96 (2010) 10–13. https://doi.org/10.1063/1.3309717.
22. W.R. Knolle, H.R. Maxwell, R.E. Benenson, Hydrogen in semi-insulating polycrystalline silicon films, J. Appl. Phys. 51 (1980) 4385–4390. https://doi.org/10.1063/1.328302.
23. A.V. Vasin, P.N. Okholin, I.N. Verovsky, A.N. Nazarov, V.S. Lysenko, K.I. Kholostov, V.P. Bondarenko, Y. Ishikawa, Study of the Processes of Carbonization and Oxidation of Porous Silicon by Raman and IR Spectroscopy, Semiconductors. 45 (2011) 350–354. https://doi.org/10.1134/S1063782611030249.

24. C. Tsai, K.H. Li, J. Sarathy, S. Shih, J.C. Campbell, B.K. Hance, J.M. White, Thermal treatment studies of the photoluminescence intensity of porous silicon, Appl. Phys. Lett. 59 (1991) 2814–2816. https://doi.org/10.1063/1.105869.
25. C.L. Chen, J. Zeng, N. Bao, H. Dai, H.Y. Gu, Oxygen backed silicon hydride in correlation with the photoluminescence of silicon nano-crystals, RSC Adv. 7 (2017) 44655–44658. https://doi.org/10.1039/c7ra02883k.
26. J.A. Luna-López, A. Morales-Sánchez, M. Aceves-Mijares, Z. Yu, C. Domínguez, Analysis of surface roughness and its relationship with photoluminescence properties of silicon-rich oxide films, J. Vac. Sci. Technol. A Vacuum, Surfaces, Film. 27 (2009) 57–62. https://doi.org/10.1116/1.3032915.
27. V.J. Mohanraj, Y. Chen, Nanoparticles - A review, Trop. J. Pharm. Res. 5 (2007) 561–573. https://doi.org/10.4314/tjpr.v5i1.14634.
28. F. Aleksandar, et al. Interventional techniques in Uro-oncology, in M. Arya, H.U. Ahmed, P. Scardino, M. Emberton. (Eds.), John Wiley & Sons, 2011, p.105-106.
29. J. Salonen, V.P. Lehto, M. Björkqvist, E. Laine, L. Niinistö, Studies of thermally-carbonized porous silicon surfaces, Phys. Status Solidi Appl. Res. 182 (2000) 123–126. https://doi.org/10.1002/1521-396X(200011)182:1<123::AID-PSSA123>3.0.CO;2-F.
30. S. Yang, W. Cai, H. Zeng, X. Xu, Ultra-fine β-SiC quantum dots fabricated by laser ablation in reactive liquid at room temperature and their violet emission, J. Mater. Chem. 19 (2009) 7119–7123. https://doi.org/10.1039/b909800c.
31. R. Intartaglia, K. Bagga, F. Brandi, G. Das, A. Genovese, E. Di Fabrizio, A. Diaspro, Optical characterization of silicon nanoparticle obtained via femtosecond laser ablation in deionized water, Synth. Photonics Nanoscale Mater. VIII. 7922 (2011) 79220P. https://doi.org/10.1117/12.882079.
32. P.G. Kuzmin, G.A. Shafeev, V. V. Bukin, S. V. Garnov, C. Farcau, R. Carles, B. Warot-Fontrose, V. Guieu, G. Viau, Silicon nanoparticles produced by femtosecond laser ablation in ethanol: Size control, structural characterization, and optical properties, J. Phys. Chem. C. 114 (2010) 15266–15273. https://doi.org/10.1021/jp102174y